

Structure and electrical properties of PZT–PMS–PZN piezoelectric ceramics

Zupei Yang*, Hui Li, Ximei Zong, Yunfei Chang

School of Chemistry and Materials Science, Shaanxi Normal University, Xi'an, 710062 Shaanxi, PR China

Received 6 April 2005; received in revised form 18 July 2005; accepted 4 August 2005

Available online 23 September 2005

Abstract

The quaternary piezoelectric ceramics of $\text{Pb}(\text{Zr}_{0.52}\text{Ti}_{0.48})\text{O}_3\text{--Pb}(\text{Mn}_{1/3}\text{Sb}_{2/3})\text{O}_3\text{--Pb}(\text{Zn}_{1/3}\text{Nb}_{2/3})\text{O}_3$ (PZT–PMS–PZN) with different PZN contents were synthesized by molten salt synthesis (MSS). The influence of PZN content on phase structure, microstructure, dielectric and piezoelectric properties was investigated in detail. The results of X-ray diffraction (XRD) show that the phase structure of ceramics transforms from rhombohedral phase to tetragonal phase with the increasing of PZN content. The morphotropic phase boundary (MPB) of composition is located in the range of PZN content from 2 to 7 mol%. The grain size of the ceramics gradually decreases with the increasing of PZN content. Dielectric and piezoelectric properties of ceramics are significantly influenced by the PZN content. Ceramics sintered at 1150 °C with 5 mol% PZN achieve excellent properties, which are as follows: $Q_m = 1381$, $K_p = 0.64$, $d_{33} = 369\text{pC/N}$, $\tan \delta = 0.0044$ and $T_c = 275^\circ\text{C}$. The PZT–PMS–PZN system is a promising material for high power piezoelectric transformers application.

© 2005 Elsevier Ltd. All rights reserved.

Keywords: Sintering; X-ray methods; Dielectric properties; Piezoelectric properties; PZT–PMS–PZN

1. Introduction

Piezoelectric ceramics have been extensively applied for actuators, ultrasonic motors, sensors and transformers. Recently, piezoelectric transformers are mainly applied to the light liquid-crystal display (LCD) backlight inverter for notebook, camcorder and PDA, etc. because piezoelectric transformers have favorable advantages, such as low profile, low power consumption and no electromagnetic noise compared with conventional electromagnetic transformers.^{1,2}

Piezoelectric transformers operated with high vibration velocity under high power convert electrical energy to mechanical vibration. Usually, mechanical quality factor Q_m is a referenced parameter of the dissipation of vibration energy. The energy loss will result in the temperature rise of the piezoelectric transformers.³ So the ceramics used for high power piezoelectric transformers should have high Q_m and low dielectric loss $\tan \delta$ to inhibit the temperature rise. In addition, the piezoelectric activity is appreciated by the value of the electromechanical

coupling factor K_p . Therefore, K_p is the figure of merit of the piezoelectric activity and the square of that gives the efficiency of the conversion of electrical-mechanical energy.^{4,5} The high K_p is required in order to increase step-up ratio of high power piezoelectric transformers. Moreover, the ceramics suitable for the application of transformers can generate large deformations. It is necessary for the materials to have high piezoelectric constant d_{33} . Accordingly, the ceramics for high power piezoelectric transformers should have a high piezoelectric constant d_{33} , a large electromechanical coupling factor K_p and a high mechanical quality factor Q_m and a low dielectric loss $\tan \delta$.

Many ternary and quaternary systems, such as PYW–PZT,⁶ PMS–PZT,⁷ PMN–PZN–PZT⁴ and PMN–PNN–PZT,⁸ have been investigated by compositional modifications or substitutions to satisfy the specific requirements of different performance devices. However, Q_m , K_p and other properties are partly concerned in the above systems, there are a few systems that can simultaneously give high d_{33} , high K_p and high Q_m and low $\tan \delta$ for high power piezoelectric transformers.

Molten salt synthesis (MSS) is believed to be a well-established process for forming pure perovskite and improving reactive activity of powders.^{9,10} According to our previous study, PZT–PMS–PZN system shows good dielectric and piezoelectric

* Corresponding author. Tel.: +86 29 8530 8205; fax: +86 29 8530 7774.
E-mail address: yangzp@snnu.edu.cn (Z. Yang).

properties. In this work, MSS method was applied to prepare the PZT–PMS–PZN powders and ceramics. The influence of PZN content on the phase structure, microstructure and electrical properties of PZT–PMS–PZN ceramics was studied in order to select the composition of ceramics with excellent dielectric and piezoelectric properties for high power piezoelectric transformers application. In addition, it is well known that CeO_2 is commonly used additive for PZT ceramics, because it improves the piezoelectric properties and decreases the dissipation factor $\tan \delta$ at the same time.¹¹ So 0.1 mol% CeO_2 was added in the compositions.

2. Experimental procedure

The powders and ceramics with compositions of $0.9\text{Pb}_{0.95}\text{Sr}_{0.05}(\text{Zr}_{0.52}\text{Ti}_{0.48})\text{O}_3-(0.1-x)\text{Pb}(\text{Mn}_{1/3}\text{Sb}_{2/3})\text{O}_3-x\text{Pb}(\text{Zn}_{1/3}\text{Nb}_{2/3})\text{O}_3+0.1\text{ mol}\% \text{CeO}_2$ were synthesized by MSS method, where $x=0.00, 0.02, 0.05, 0.07$, and 0.10 , respectively. Reagent-grade oxide powders Pb_3O_4 (97%), ZrO_2 (99%), TiO_2 (98%), Nb_2O_5 (99.5%), CeO_2 (99.5%), SrCO_3 (99%), ZnO (99%), Sb_2O_3 (99%), MnO_2 (90%) and the molten salts (NaCl-KCl) were mixed, respectively. The mixtures were ball-milled in ethanol for 10 h, and then dried at 80°C . The powders were calcined at 780°C for 2 h and then were washed with hot distilled water for several times until Cl^- ions could not be detected by Ag^+ reagent. The calcined powders were dried at 80°C . After drying, powders were added with 5 wt.% poly vinyl alcohol (PVA) solution, and then were pressed into pellets with 13 mm in diameter under a pressure of 100 MPa. Pellets were sintered at $1100\text{--}1170^\circ\text{C}$ for 4 h in a sealed alumina crucible with lead atmosphere.

Subsequently sintered discs were polished and silver-paste electrodes were fired at 560°C , respectively. The samples for the piezoelectric properties measurements were poled in the silicone oil at 120°C by applying a dc electric field of 3 kV/mm for 30 min.

The phase structure of the calcined powders and sintered ceramics was analyzed using an X-ray diffraction (XRD, Model DMX-2550/PC, Rigaku, Japan) with a 2θ range from 10° to 70° . Surface microstructure was observed using a scanning electron microscopy (SEM, Model Quanta 200, FEI Company). Dielectric properties were obtained by measuring the capacitance and dielectric loss at 1 kHz at room temperature by using an LCR meter (HP 4294A). The Curie temperature (T_c) was determined by temperature dependence of the dielectric constant at 1 kHz. The piezoelectric constants (d_{33}) were measured using a quasi-static piezoelectric d_{33} meter (Model ZJ-3d, Institute of Acoustics Academic Sinica, China). The electromechanical coupling factor (K_p) and mechanical quality factor (Q_m) were determined by the resonance and anti-resonance technique on the basis of IEEE standards using an impedance analyzer (HP4294A), and the calculation equations are as follows: $K_p = [2.51(f_a - f_r)f_r^{-1}]^{1/2}$ and $Q_m = f_a^2[2\pi R_f C f_r(f_a^2 - f_r^2)]^{-1}$, where f_r and f_a are resonant and anti-resonant frequencies (Hz), and R_f and C are resonant impedance (ohms) and electrical capacitance (farads).

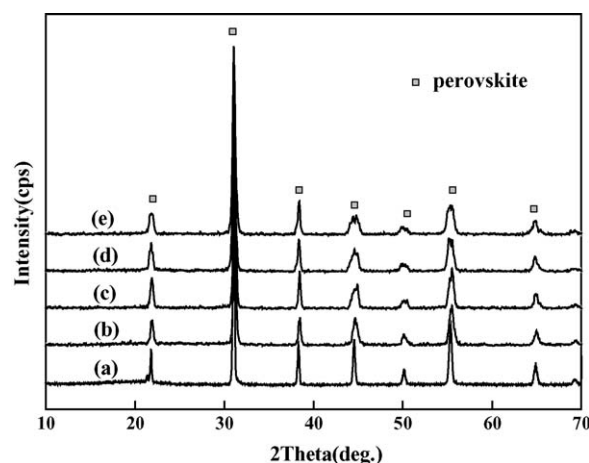


Fig. 1. The XRD patterns of powders calcined at 780°C with different PZN contents, where (a) $x=0.00$, (b) $x=0.02$, (c) $x=0.05$, (d) $x=0.07$, and (e) $x=0.10$.

3. Results and discussion

3.1. Phase structure

Figs. 1 and 2 show the XRD patterns of the powders calcined at 780°C and the ceramics sintered at 1150°C with different PZN contents, respectively. It can be seen that all the powders are pure perovskite phase without pyrochlore phase. The ceramics with various PZN contents all exist as pure perovskite phase. The ceramics exist as rhombohedral phase which is indicated by the single $(200)_R$ peak at $x=0.00$. As PZN content increases from 2 to 7 mol%, the ceramics coexist as tetragonal and rhombohedral phase revealed by the coexistence of $(002)_T$ and $(200)_R$ peaks in the 2θ range from 43.8° to 45.3° . The ceramics with $x=0.10$ exist as tetragonal phase revealed by the splitting of $(002)_T$ and $(200)_T$ peaks in the 2θ range from 43.5° to 45.4° . According to the results of Fig. 2, the system transforms from rhombohedral phase to tetragonal phase with the increasing of PZN content. It is clear that the MPB exists in the range of PZN content from 2 to 7 mol%.

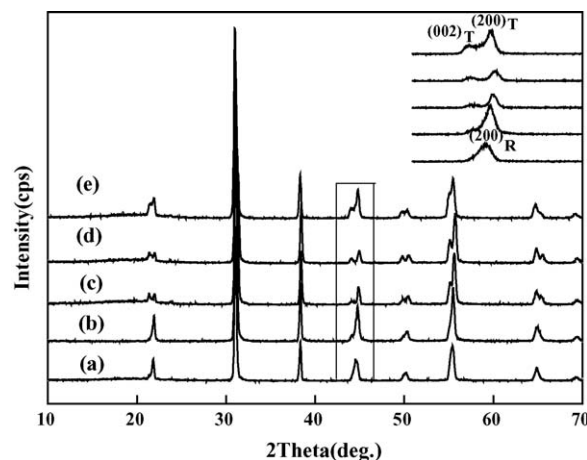


Fig. 2. The XRD patterns of ceramics sintered at 1150°C with different PZN contents, where (a) $x=0.00$, (b) $x=0.02$, (c) $x=0.05$, (d) $x=0.07$, and (e) $x=0.10$.

3.2. Microstructure

Fig. 3 shows the SEM micrographs of PZT–PMS–PZN ceramics sintered at 1150 °C with various PZN contents. It can clearly be seen that the grain size gradually decreases with the increasing of PZN content. It is mainly attributed to the solubility of PZN in the PZT–PMS system. PZN has certain solubility value in the PZT–PMS composition matrix, but further addition of PZN beyond the solubility limit will inhibit the grain growth due to segregation of PZN at the grain boundary.¹²

3.3. Piezoelectric and dielectric properties

Fig. 4 shows piezoelectric constant d_{33} , mechanical quality factor Q_m and electromechanical coupling factor K_p of ceramics sintered at 1150 °C as a function of PZN content. It can be seen that PZN content strongly influences piezoelectric constant d_{33} . With the increasing of PZN content, piezoelectric constant d_{33} abruptly increases. But when PZN content is beyond 7 mol%, piezoelectric constant d_{33} slowly changes. The maximum 415 pC/N of piezoelectric constant d_{33} is obtained at

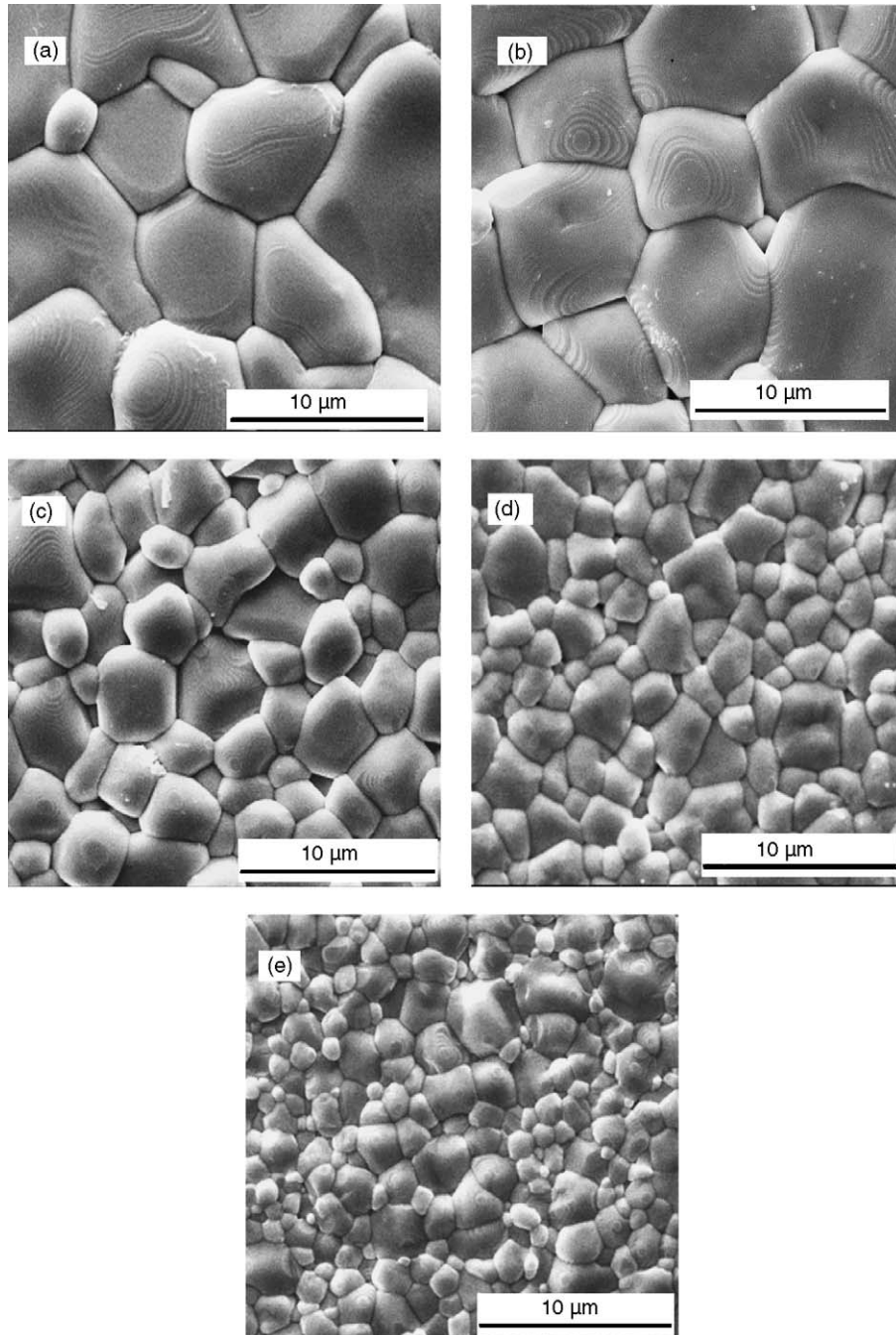


Fig. 3. The SEM micrographs ($\times 6000$) of ceramics sintered at 1150 °C with different PZN contents, where (a) $x=0.00$, (b) $x=0.02$, (c) $x=0.05$, (d) $x=0.07$, and (e) $x=0.10$.

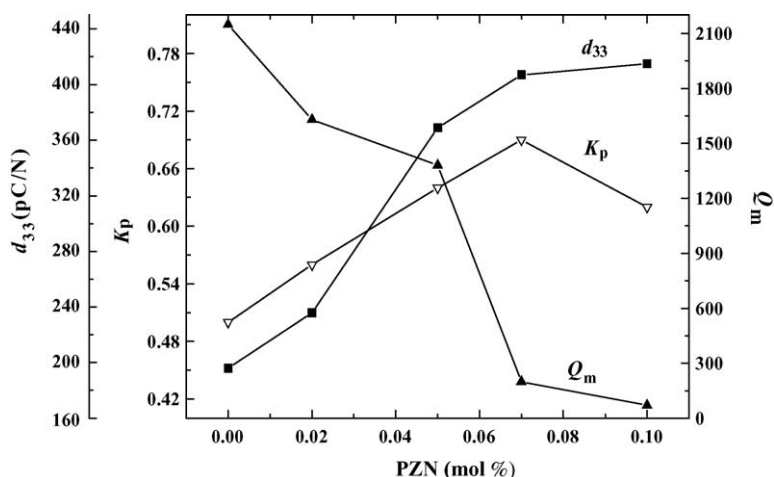


Fig. 4. d_{33} , K_p and Q_m of ceramics sintered at 1150 °C as a function of PZN content.

$x=0.10$. These variations may be attributed to the transformation of phase structure. As PZN content increases, the ceramics transform from rhombohedral phase to tetragonal phase. Piezoelectric constant d_{33} achieves the optimized value at the MPB. In addition, K_p sharply increases at first with the increasing of PZN content. When $x>0.07$, K_p shows a tendency of decreasing. The K_p maximum of 0.69 is obtained at $x=0.07$. Q_m strongly drops with the increasing of PZN content, especially in the range of PZN content from 5 to 7 mol%, which is attributed to the addition of PZN with a relative low Q_m value. According to the above results, the composition at $x=0.05$ shows the optimized values of d_{33} , K_p and Q_m , which are 369 pC/N, 0.64 and 1381, respectively.

Fig. 5 shows dielectric loss $\tan \delta$ of ceramics sintered at 1150 °C as a function of PZN content. Dielectric loss $\tan \delta$ slowly decreases at first, and begins to increase when PZN content is up to 5 mol%. Using thermodynamic method that utilizes the expression for the energy of the piezoelectric ceramics system, linear relation between Q_m^{-1} and $\tan \delta$ has established.^{13,14} From Figs. 4 and 5, the relation between Q_m and $\tan \delta$ is obviously correlated, especially for the PZN content above 5 mol%. There is a minimum of $\tan \delta$ at $x=0.05$ with 0.0044, and Q_m reaches the higher value at the same time. For applying piezoelectric

ceramics in piezoelectric transformers, low $\tan \delta$ and high Q_m are necessary to for suppressing the generation of heat during operation.

Fig. 6 shows the dielectric constant ϵ_r of the unpoled and poled ceramics sintered at 1150 °C as a function of PZN content. It is observed that the dielectric constant ϵ_r of the poled ceram-

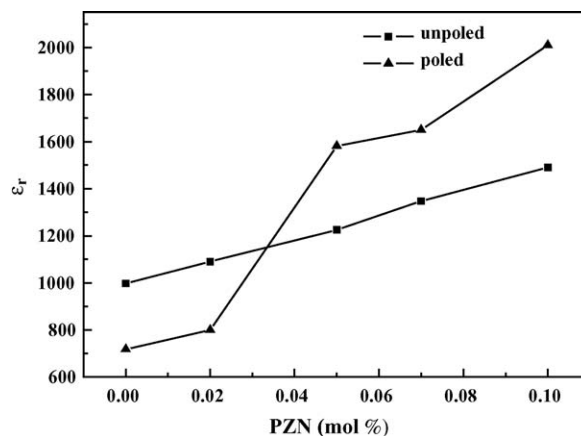


Fig. 6. ϵ_r of the unpoled and poled ceramics sintered at 1150 °C as a function of PZN content.

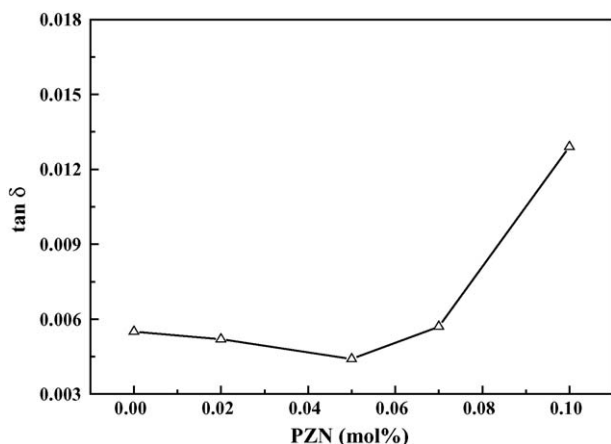


Fig. 5. $\tan \delta$ of ceramics sintered at 1150 °C as a function of PZN content.

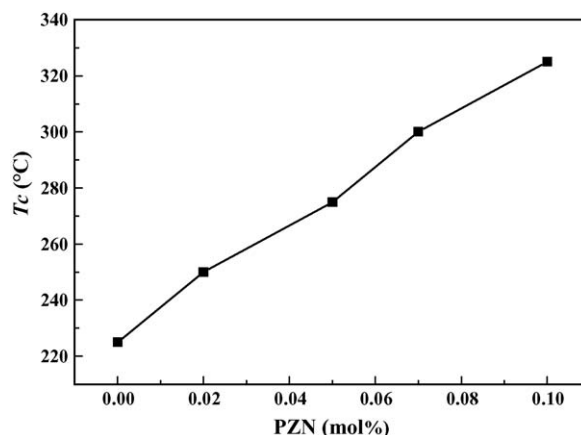


Fig. 7. T_c of ceramics sintered at 1150 °C as a function of PZN content.

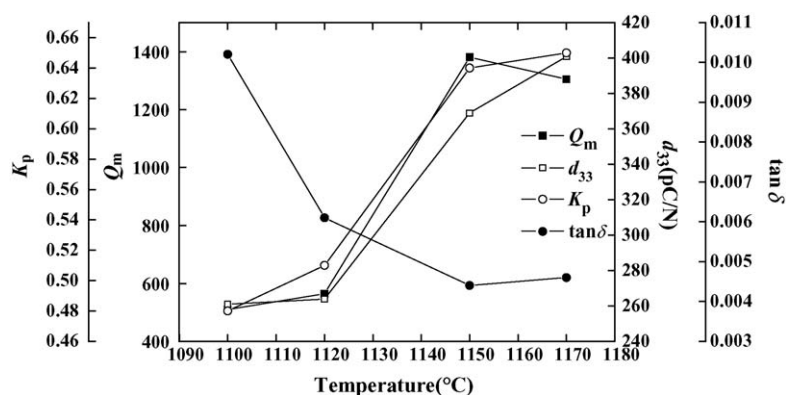


Fig. 8. d_{33} , K_p , Q_m and $\tan \delta$ of ceramics with $x=0.05$ as a function of sintering temperature.

ics and unpoled ceramics show the similar tendency of increase with the increasing of PZN content. $\Delta\epsilon_r = (\epsilon_r^{\text{poled}} - \epsilon_r^{\text{unpoled}})$ value is negative for x below 0.03 and $\Delta\epsilon_r$ is positive for x above 0.03. From the results of XRD, the MPB is in the range of 2–7 mol% PZN content, in which the ceramics coexist as tetragonal and rhombohedral phase. When x sites in 0.02–0.03, the rhombohedral phase is dominant in the ceramics. But when x sites in 0.03–0.07, the tetragonal phase is dominant. The relationship between the phase transition and the $\Delta\epsilon_r$ changes is similar with that previously observed by Hou.¹⁵

Fig. 7 shows the Curie temperature T_c of ceramics sintered at 1150 °C as a function of PZN content. To avoid the transition from ferroelectric to paraelectric state occurring in the operating temperature range for piezoelectric transformers, the high Curie temperature of 250 °C or more is also needed for piezoelectric materials. It can be seen that the Curie temperature T_c sharply increases with the increasing of PZN content. The Curie temperature of the composition with $x=0.05$ is 275 °C, which can contribute to the stability of the material characteristics in operating.

Taking into account the above results, the PZT–PMS–PZN ceramics with different PZN contents have been investigated and the composition with $x=0.05$ is selected for its excellent dielectric and piezoelectric properties. In order to further optimize properties and the processing route, the properties of the ceramics with the composition of 0.90PZT–0.05PMS–0.05PZN at different sintering temperature are studied.

Fig. 8 shows piezoelectric and dielectric properties of the sintered ceramics with $x=0.05$ as a function of sintering temperature. It can be seen that piezoelectric constant d_{33} slowly varies in the sintering temperature range from 1100 to 1120 °C. Increasing the sintering temperature above 1120 °C, piezoelectric constant d_{33} rapidly rises and gets the maximum at 1170 °C. When sintering temperature increases, Q_m markedly increases at first, and then decreases. Moreover, Q_m value reaches the maximum at the sintering temperature of 1150 °C. K_p greatly increases in the range of sintering temperature from 1100 °C to 1150 °C. Increasing the sintering temperature above 1150 °C, K_p slightly rises and obtains the maximum of 0.65 at 1170 °C. $\tan \delta$ sharply decreases with the increasing of PZN content below 1150 °C. Above 1150 °C, $\tan \delta$ slightly changes and the lower value is obtained at 1150 °C. In conclusion, the suitable sintering

temperature of this material is 1150 °C. Moreover, the dielectric and piezoelectric properties corresponding to this sintering temperature could make material a candidate for the demand of piezoelectric transformers application.

4. Conclusions

PZT–PMS–PZN ceramics of pure perovskite structure were synthesized via MSS. The phase structure of system transformed from single rhombohedral to tetragonal in the range of $0.00 \leq x \leq 0.10$. The morphotropic phase boundary of composition existed in the range of $0.02 \leq x \leq 0.07$. Microstructure showed the grain size markedly decreased with the increasing of PZN content. As PZN content increased, K_p increased and then decreased, d_{33} and T_c sharply increased, at the same time $\tan \delta$ decreased and then increased, while Q_m gradually dropped. Meanwhile, K_p , d_{33} , Q_m and $\tan \delta$ was influenced by the sintering temperature. Taking into account electrical properties and sintering temperature, the ceramics with composition of 0.90PZT–0.05PMS–0.05PZN sintered at 1150 °C have desirable dielectric and piezoelectric prosperities. The optimum values of Q_m , K_p , d_{33} , $\tan \delta$ and T_c were 1381, 0.64, 369pC/N, 0.0044 and 275 °C, respectively, which shows that the 0.90PZT–0.05PMS–0.05PZN material is a good candidate for piezoelectric transformers application.

References

- Shin, H., Ahn, H. and Han, D. Y., Review modeling and analysis of multilayer piezoelectric transformer. *Mater. Chem. Phys.*, 2005, **92**, 616–620.
- Fuda, Y., Kumasaka, K., Katsuno, M., Sato, H. and Ino, Y., Piezoelectric transformer for cold cathode fluorescent lamp inverter. *Jpn. J. Appl. Phys.*, 1997, **36**, 3050–3052.
- Gao, Y., Chen, Y. H., Ryu, J., Uchino, K. and Viehland, D., Eu and Yb substituent effects on the properties of $\text{Pb}(\text{Zr}_{0.52}\text{Ti}_{0.48})\text{O}_3$ – $\text{Pb}(\text{Mn}_{1/3}\text{Sb}_{2/3})\text{O}_3$ ceramics: development of a new high-power piezoelectric with enhanced vibrational velocity. *Jpn. J. Appl. Phys.*, 2001, **40**, 687–693.
- Wang, C. H., The piezoelectric and dielectric properties of PZT–PMN–PZN. *Ceram. Int.*, 2004, **30**, 605–611.
- Hartal, K. H., Physics of ferroelectric ceramics used in electronic devices. *Ferroelectrics*, 1976, **12**, 9–19.
- Yoon, S. J., Joshi, A. and Uchino, K., Effect of additives on the electromechanical properties of $\text{Pb}(\text{Zr,Ti})\text{O}_3$ – $\text{Pb}(\text{Y}_{2/3}\text{W}_{1/3})\text{O}_3$ ceramics. *J. Am. Ceram. Soc.*, 1997, **80**, 1035–1039.

7. Gao, Y. K., Uchino, K. and Viehland, D., Effects of rare earth metal substituents on the piezoelectric and polarization properties of $\text{Pb}(\text{Zr,Ti})\text{O}_3\text{--Pb}(\text{Sb,Mn})\text{O}_3$ ceramics. *Jpn. J. Appl. Phys.*, 2002, **92**(4), 2094–2099.
8. Gui, Z. L., Li, L. T., Lin, H. Q. and Zhang, X. W., Low temperature sintering of lead magnesium nickel niobate zirconate titanate(PMN–PNN–PZT)piezoelectric ceramic, with high performances. *Ferroelectrics*, 1990, **101**, 93–99.
9. Yoon, K. H., Cho, Y. S. and Kang, D. H., Review molten salt synthesis of lead-based relaxors. *J. Mater. Sci.*, 1998, **33**, 2977–2984.
10. Yang, Z., Chang, Y., Zong, X. and Zhu, J., Preparation and properties of PZT–PMN–PMS ceramics by molten salt synthesis. *Mater. Lett.*, 2005, **59**(22), 2790–2793.
11. Wang, X., Chan, H. L. W. and Choy, C. L., Piezoelectric and dielectric properties of CeO_2 -added $(\text{Bi}_{0.5}\text{Na}_{0.5})_{0.94}\text{Ba}_{0.06}\text{TiO}_3$ lead-free ceramics. *Solid State Commun.*, 2003, **125**, 395–399.
12. Yoo, J., Lee, Y., Yoon, K., Hwang, S., Suh, S., Kim, J. and Yoo, C., Microstructural, electrical properties and temperature stability of resonant frequency in $\text{Pb}(\text{Ni}_{1/2}\text{W}_{1/2})\text{O}_3\text{--Pb}(\text{Mn}_{1/3}\text{Nb}_{2/3})\text{O}_3\text{--Pb}(\text{Zr,Ti})\text{O}_3$ ceramics for high-power piezoelectric transformer. *Jpn. J. Appl. Phys.*, 2001, **40**, 3256–3259.
13. Chen, C. Y. and Lin, H. L., Piezoelectric properties of $\text{Pb}(\text{Mn}_{1/3}\text{Nb}_{2/3})\text{O}_3\text{--PbZrO}_3\text{--PbTiO}_3$ ceramics with sintering aid of $2\text{CaO--Fe}_2\text{O}_3$ compound. *Ceram. Int.*, 2004, **30**(8), 2075–2079.
14. Wang, M. C., Huang, M. S. and Wu, N. C., Effects of $30\text{B}_2\text{O}_3\text{--}25\text{Bi}_2\text{O}_3\text{--}45\text{CdO}$ glass addition on the sintering of $12\text{Pb}(\text{Ni}_{1/3}\text{Sb}_{2/3})\text{O}_3\text{--}40\text{PbZrO}_3\text{--}48\text{PbTiO}_3$ piezoelectric ceramics. *J. Euro. Ceram. Soc.*, 2001, **21**, 695–701.
15. Hou, Y. D., Zhu, M. K., Tian, C. S. and Yan, H., Structure and electrical properties of PMZN–PZT quaternary ceramics for piezoelectric transformers. *Sens. Actuators A*, 2004, **116**, 455–460.